

# Simultaneous SAXS/WAXS and d.s.c. analysis of the melting and recrystallization behaviour of quenched polypropylene

W. J. O'Kane, R. J. Young\* and A. J. Ryan

*Polymer Science and Technology Group, University of Manchester/UMIST, Manchester M60 1QD, UK*

and W. Bras†, G. E. Derbyshire and G. R. Mant

*SERC Daresbury Laboratory, Warrington, Cheshire WA4 4AD, UK*

*(Received 19 March 1993; revised 2 August 1993)*

The behaviour of a quenched ethylene-propylene block copolymer cast film has been investigated during melting and recrystallization experiments carried out at heating and cooling rates of  $10^{\circ}\text{C min}^{-1}$ . The experimental techniques used to follow the melting and recrystallization processes were differential scanning calorimetry (d.s.c.) and simultaneous small-angle X-ray scattering (SAXS) and wide-angle X-ray scattering (WAXS). In particular, the WAXS results show that the melting of the material is preceded by a solid-state transition involving transformation of the quenched structure into the monoclinic  $\alpha$  modification. This transition appears as an exotherm in the range  $65\text{--}120^{\circ}\text{C}$  on the d.s.c. melting trace. SAXS results show that an increase in the amount of long-range order occurs during this transition. The sample was then found to melt at  $162^{\circ}\text{C}$ . Upon cooling from the melt, recrystallization of the monoclinic  $\alpha$  modification was found to occur in the range  $123\text{--}105^{\circ}\text{C}$  without any apparent prior formation of the quenched structure.

**(Keywords: quenched polypropylene; monoclinic polypropylene; synchrotron radiation)**

## INTRODUCTION

Since Natta discovered that propylene could be polymerized into a semicrystalline polymer, the structure of isotactic polypropylene (PP) has been studied extensively<sup>2-5</sup>. The monoclinic  $\alpha$  form, described by Natta<sup>2</sup>, predominates and a typical wide-angle X-ray scattering (WAXS) scan of this form is shown in *Figure 1*.

Upon rapid quenching from the melt, a disordered phase of PP is obtained, intermediate in order between the amorphous and crystalline phases. The structure of this phase has not yet been fully resolved. Natta *et al.*<sup>6</sup> have described this phase as 'smectic'. Miller<sup>7</sup> and Corradini *et al.*<sup>8</sup> have both suggested that this phase is essentially paracrystalline, exhibiting no long-range order. Gailey and Ralston<sup>9</sup> and Gesovich and Geil<sup>10</sup> have proposed that the quenched form consists of very fine crystallites of the hexagonal  $\beta$  phase of PP. Bodor *et al.*<sup>11</sup>, however, assumed that the quenched form contained monoclinic PP and concluded that crystal-size line broadening was responsible for the characteristic WAXS pattern, examples of which are shown in *Figure 2*. Recently<sup>12</sup>, the quenched phase has been described as 'condis crystal'.

Although the quenched form of PP is stable at room temperature, it transforms to the monoclinic crystal form on heating at temperatures above  $70\text{--}80^{\circ}\text{C}$ <sup>12-15</sup>. Evidence has been obtained mostly by X-ray diffraction analysis

of samples at ambient temperatures following heat treatments at elevated temperatures. This transition from quenched to monoclinic  $\alpha$  modification can also be observed on differential scanning calorimetry (d.s.c.) traces obtained from the melting of quenched PP. An exothermic d.s.c. peak is seen as the sample is heated above  $80^{\circ}\text{C}$ <sup>14-16</sup>. Vittoria<sup>15</sup> has stated that this exotherm is due to the upper glass transition which has been suggested<sup>17</sup> for isotactic polypropylene. On annealing of the quenched form an endotherm appears on the d.s.c. trace<sup>15,18</sup>. Zannetti *et al.*<sup>18</sup> have reported that a 'predominantly intramolecular transformation due to recoiling of segments having different lengths and different ternary helix spiralization is occurring and that the peak is due to melting of small crystalline regions formed by annealing'. They suggested that these regions melt at temperatures which depend on their dimensions and order as a consequence of the thermal treatments of the samples.

Although X-ray diffraction and d.s.c. analysis have been carried out in order to monitor phase transformations during the heat treatments and melting of quenched PP, results from the two techniques have not been correlated closely to one another. In addition, very few results have been published on this transition with respect to small-angle X-ray scattering (SAXS). The object of this paper is to report the results obtained from simultaneous SAXS/WAXS and d.s.c. experiments carried out under similar conditions on samples of quenched PP film designed to monitor the transition from quenched to monoclinic  $\alpha$  modification in detail.

\* To whom correspondence should be addressed

† The Netherlands Research Organization (NWO)

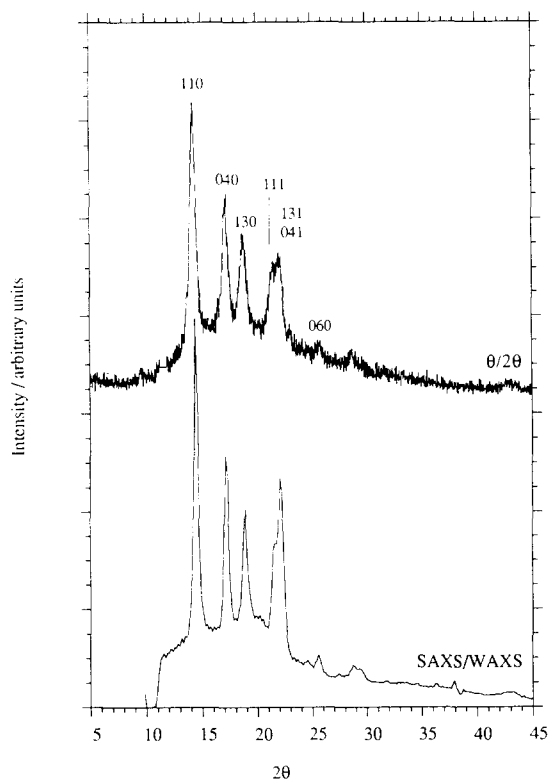


**Figure 1** Typical WAXS diffraction patterns of the monoclinic  $\alpha$  modification of isotactic polypropylene obtained using  $\theta/2\theta$  and SAXS/WAXS cameras

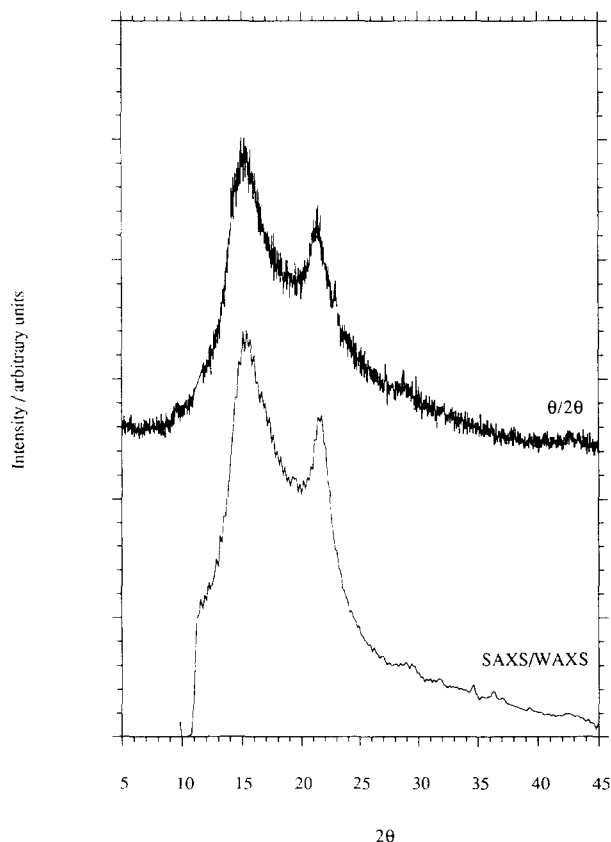


**Figure 2** Typical WAXS diffraction patterns of the quenched modification of isotactic polypropylene obtained using  $\theta/2\theta$  and SAXS/WAXS cameras

## EXPERIMENTAL

### Materials

The material studied in the experiments was an ethylene-propylene block copolymer containing  $\sim 7\%$  ethylene. The polymer had been manufactured commercially by casting (chill roll temperature  $\sim 20^\circ\text{C}$ ), which resulted in the production of a  $50\ \mu\text{m}$  thick film with the structure shown in *Figure 2*. The film was defined by the manufacturers as medical grade, the polymer used to manufacture the film having virtually no additives such as fillers, nucleating agents, etc.

### SAXS/WAXS experiments

The static X-ray diffraction experiments were carried out at UMIST using a Philips horizontal powder X-ray diffractometer system using Ni-filtered  $\text{CuK}\alpha$  radiation. The diffraction scans were collected over a period of  $\sim 20$  min between  $2\theta$  values of  $5^\circ$  and  $45^\circ$  using a step size of  $0.025^\circ$ .

Simultaneous SAXS/WAXS measurements were undertaken on beamline 8.2 of the SRS at the SERC Daresbury Laboratory, Warrington, UK. Details of the storage ring, the radiation and camera geometry and the data collection electronics have been given in detail elsewhere<sup>19</sup>. The camera was equipped with a multiwire quadrant detector (SAXS) located  $\sim 3.5$  m from the sample position and a curved knife-edge detector (WAXS) that covered  $120^\circ$  of arc at a radius of 0.4 m. A vacuum chamber was placed between the sample and detectors in order to reduce air scattering and absorption. Both the exit window of the beamline and the entrance window of the vacuum chamber were made from  $15\ \mu\text{m}$  mica; the exit windows of the vacuum chambers were made from  $15\ \mu\text{m}$  mylar film and  $10\ \mu\text{m}$  Kapton film for the WAXS and SAXS detectors, respectively. The WAXS detector had a spatial resolution of  $50\ \mu\text{m}$  and could handle up to  $\sim 100\ 000$  counts  $\text{s}^{-1}$ ; only  $90^\circ$  of arc were active in these experiments, the rest of the detector being shielded with lead. A beamstop was mounted just before the SAXS exit window to prevent the direct beam from hitting the SAXS detector, which measured intensity in the radial direction (over an opening angle of  $70^\circ$  and an active length of 0.2 m) and was only suitable for isomorphous scatterers. It had an advantage over single-wire detectors in that the active area increased radially, improving the signal to noise ratio. The spatial resolution of the SAXS detector was  $500\ \mu\text{m}$  and it could handle up to  $\sim 250\ 000$  counts  $\text{s}^{-1}$ .

The specimens for SAXS/WAXS were prepared by placing a stack of four discs,  $50\ \mu\text{m}$  thick and  $\sim 8$  mm diameter polymer sheets, in a cell comprising a Du Pont d.s.c. pan fitted with windows ( $\sim 7$  mm diameter) made from  $5\ \mu\text{m}$  thick mica. The modified d.s.c. pans are described elsewhere<sup>20</sup>. Loaded, sealed pans were glued to a J-type thermocouple and placed in a spring-loaded holder in a Linkam TMH600 hot-stage mounted on the optical bench. The silver heating block of the hot-stage contained a  $4 \times 1$  mm conical hole which allowed the transmitted and scattered X-rays to pass through unhindered. A nominal heating rate of  $10^\circ\text{C min}^{-1}$  was used. Owing to the nature of the furnace there was a temperature drift across the sample chamber which necessitated direct measurement of the temperature at the sample position in addition to the temperature monitoring and control of the furnace.

The scattering pattern from an oriented specimen of wet collagen (rat-tail tendon) was used to calibrate the SAXS detector and high density polyethylene, aluminium and an NBS silicon standard were used to calibrate the WAXS detector. A parallel-plate ionization detector placed before the sample cell recorded the incident intensities. The experimental data were corrected for background scattering (subtraction of the scattering from the camera, hot-stage and an empty cell), sample thickness and transmission, and the positional alinearity of the detectors.

#### D.s.c. experiments

A Du Pont 2000 thermal analysis system equipped with a 910 d.s.c. cell was used for heat flow measurements to examine the polypropylene quenched to monoclinic transition temperature  $T_{sm}$ , melting temperature  $T_m$  and recrystallization temperature  $T_c$ . The values reported were taken at the peak of the transition. To reproduce the SAXS/WAXS conditions, sample masses of 3.5 mg were used in Du Pont d.s.c. pans at a heating rate of  $10^\circ\text{C min}^{-1}$ . The purge gas used was dry nitrogen.

## RESULTS AND DISCUSSION

Figures 1 and 2 show comparative patterns obtained from a typical X-ray diffraction (XRD) apparatus (Philips  $\theta/2\theta$  camera) and the SAXS/WAXS apparatus on beamline 8.2 at Daresbury. The  $\theta/2\theta$  scans were obtained over a period of 20 min, with the intensity being recorded every  $0.025^\circ$  ( $2\theta$ ). In contrast, the SAXS/WAXS diffraction patterns were obtained in 10 s, with the intensity of the pattern being recorded every  $0.175^\circ$  ( $2\theta$ ). The SAXS/WAXS camera does not have the angular resolution of the  $\theta/2\theta$  apparatus, but the scans obtained by the SAXS/WAXS apparatus are of superior resolution to the  $\theta/2\theta$  camera because: (i) the signal to noise ratio is

improved; and (ii) the divergence of the X-ray beam is much smaller (0.25 mrad compared to 14.0 mrad for the  $\theta/2\theta$  camera).

The time-resolved WAXS synchrotron radiation scan obtained from the melting and recrystallization experiment on the PP film is illustrated in Figure 3. The figure is a plot of intensity  $I(2\theta, T)$  versus scattering angle  $2\theta$  versus temperature  $T$  during heating and cooling at  $1.67^\circ\text{C}$  per scan in the temperature range  $20^\circ\text{C}$  to  $200^\circ\text{C}$  to  $20^\circ\text{C}$ . Only every other frame was plotted so that the individual traces could be clearly distinguished from one another. From the figure it can be seen that the melting of the film occurs by a two-stage process: (i) a transition from quenched to monoclinic  $\alpha$  modification occurring at temperatures above  $60^\circ\text{C}$ ; and (ii) subsequent melting of the monoclinic crystallites.

Recrystallization appears to occur by a single-stage process, this involving the formation of the monoclinic phase as the sample is cooled to below  $125^\circ\text{C}$  at  $10^\circ\text{C min}^{-1}$ . This is as expected as the quenched form is only obtained upon rapid cooling from the melt<sup>21</sup>.

The SAXS data collected along with the WAXS data during the melting and recrystallization experiments are shown in Figure 4 as a three-dimensional plot of intensity  $I(q, T)$  versus scattering vector  $q = (4\pi/\lambda) \sin(\theta/2)$ , where  $\theta$  is the scattering angle, versus temperature  $T$ . SAXS analysis yields information about structures with dimensions 10–1000 times larger than those revealed by WAXS, i.e. superstructures of 1–100 nm in size. In solid synthetic polymers stacks of crystalline lamellae, microfibrils and often macromolecular-like entities build up structures of a certain regularity which give rise to discrete maxima in the SAXS curve<sup>22</sup>. Initially, at room temperature a featureless SAXS pattern is obtained (Figure 4), indicating that the quenched form exhibits no long-range order and a small electron density fluctuation. As the sample is heated to above  $65^\circ\text{C}$  (where the transition from

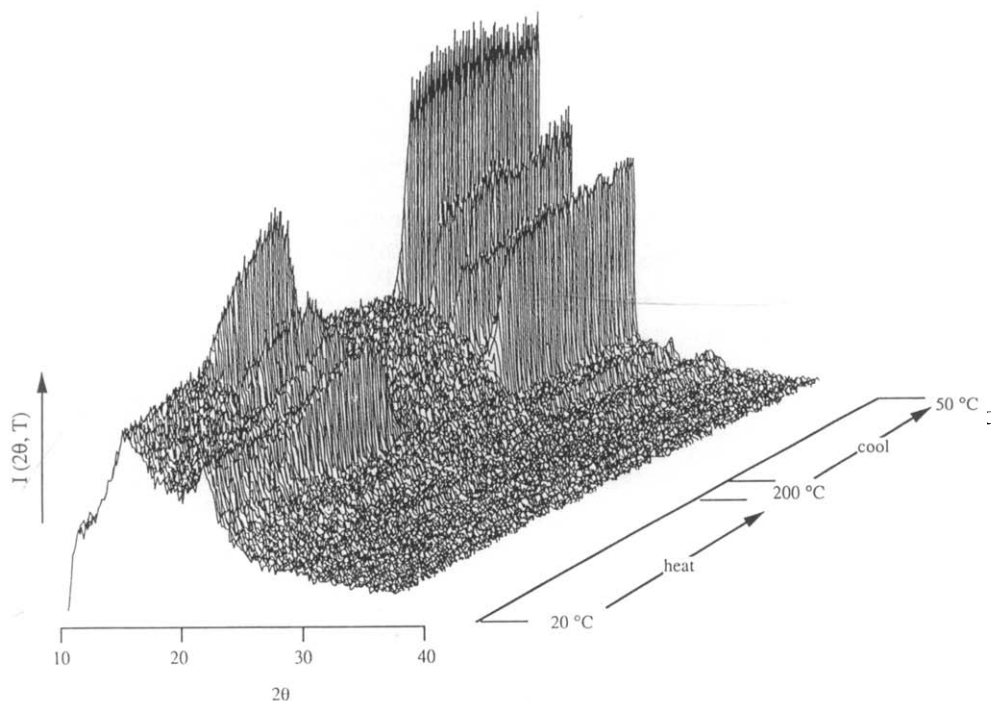


**Figure 3** Three-dimensional plot of intensity  $I(2\theta, T)$  versus scattering angle  $2\theta$  ( $5^\circ < 2\theta < 45^\circ$ ) versus temperature  $T$  in the range  $20^\circ\text{C}$  to  $200^\circ\text{C}$  to  $50^\circ\text{C}$  obtained during the melting and recrystallization of the quenched form of PP

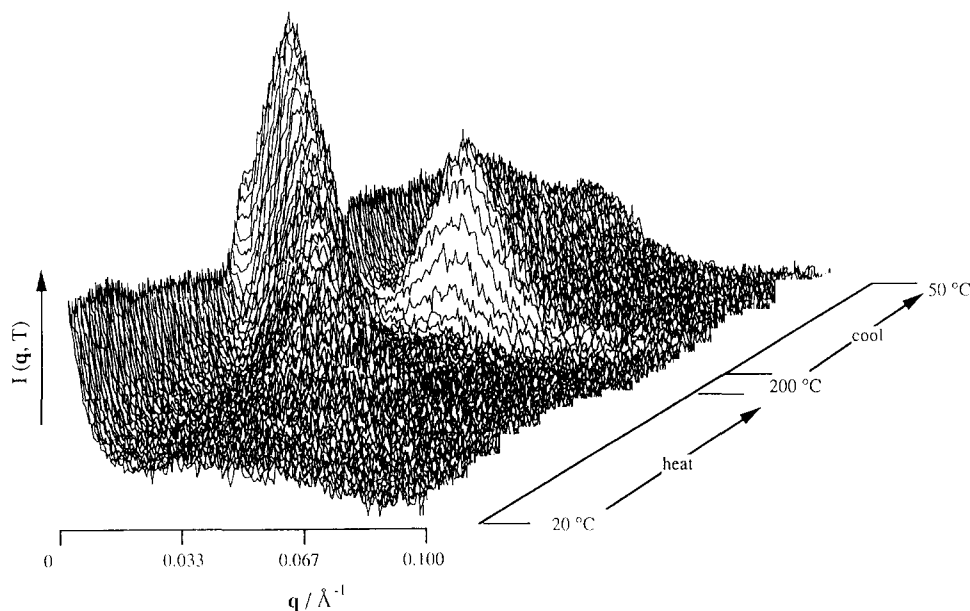


**Figure 4** Three-dimensional plot of intensity  $I(q, T)$  versus scattering vector  $q$  ( $0 < q < 0.1 \text{ \AA}^{-1}$ ) versus temperature  $T$  in the range  $20^\circ\text{C}$  to  $200^\circ\text{C}$  to  $50^\circ\text{C}$  obtained during the melting and recrystallization of the quenched form of PP

quenched to monoclinic begins to occur), the order in the sample increases (indicated by the appearance of a peak on the SAXS pattern). This order increases as the temperature is raised and is characterized by the peak position in the Lorentz-corrected scattering pattern shifting from  $q = 0.06 \text{ \AA}^{-1}$  to  $q = 0.02 \text{ \AA}^{-1}$  (Figure 5a). This corresponds to a change in the  $d$  spacing from  $105 \text{ \AA}$  to  $310 \text{ \AA}$  ( $d = 2\pi/q^*$ , where  $q^*$  corresponds to the maximum in the Lorentz-corrected  $I(q)q^2$  versus  $q$  curve), indicating that the long-range order increases as the transition from quenched to monoclinic proceeds. The long-range order then disappears completely as the sample is melted. The continuous shift in the SAXS pattern is consistent with a dynamic crystal structure which is continuously reorganizing by lamellar thickening.

Upon recrystallization the sample exhibits long-range order. However, in this case once the long-range order is obtained, the  $d$  spacing essentially remains constant at  $d = 186 \text{ \AA}$  between  $123^\circ\text{C}$  and  $23^\circ\text{C}$  (Figure 5b), indicating that the formation of the monoclinic  $\alpha$  modification is the major process occurring during crystallization at  $10^\circ\text{C min}^{-1}$  and that it is this phase which results in the long-range order observed in the sample. Further cooling of the sample to room temperature increases the amount of monoclinic phase present in the polymer, but does not alter the macroscopic characteristics of the polymer structure.

The melting and recrystallization results can also be analysed quantitatively in terms of the invariant<sup>22</sup>

$$Q = \frac{1}{2\pi i_e} \int_0^\infty I(q)q^2 dq = \frac{1}{2\pi i_e} k\phi \langle 1 - \phi \rangle (\eta_1 - \eta_2)^2 \quad (1)$$

where  $\phi$  is the fractional crystallinity of the sample,  $\eta_1$  is the electron density in the crystalline phase,  $\eta_2$  is the electron density in the amorphous phase and  $i_e$  is the Thompson scattering factor. The quantity  $Q$  is known as the invariant (being independent of the size or shape of structural inhomogeneities). The absolute value of the invariant requires absolute intensity measurements, thermal background subtraction, and extrapolation to

$q = 0$  and  $q = \infty$ , and so is computationally difficult to achieve. In practice, a relative invariant  $Q'$  is calculated by summation of the area under the  $I(q)q^2$  versus  $q$  curve between the first reliable data point and the region in which  $I(q)q^2$  becomes constant. Owing to the relative nature of the intensity measurement, the value of  $Q'$  is also only relative with arbitrary units.

For the PP sample studied  $Q'$  was calculated by integration between  $q = 0.02 \text{ \AA}^{-1}$  and  $q = 0.15 \text{ \AA}^{-1}$  and the relative invariant as a function of time is shown in Figure 6. Although it is only a relative measurement, it can be seen from equation (1) that the invariant will have a maximum value at 50% crystallinity. Thus, as Figure 6 shows, the invariant increases (and hence the degree of crystallinity through the transition from quenched to monoclinic) as the temperature increases before falling off rapidly as the sample melts, when any structure which had existed is lost. As the invariant did not decrease at any stage prior to melting it is assumed that although the crystal perfection of the PP was increasing, the sample ultimately did not attain 50% crystallinity. Upon cooling, the relative invariant increases as the sample crystallizes into the monoclinic  $\alpha$  modification and then decreases as crystallization proceeds, resulting in a sample which has a crystallinity greater than 50%. It should be noted, however, that although the relative invariant can detect changes in crystallinity it cannot by itself detect and monitor the actual transition from quenched to monoclinic, the growth in  $Q'$  being continuous. The differences in the values of  $Q'_{\text{max}}$  for the melting and recrystallization processes are due to changes in the sample thickness caused by the melting of the specimen, and could not be readily corrected for with the current experimental set-up.

The WAXS integrated intensity of the peak at  $\sim 22^\circ$  (a combination of (111) and (131)/(041), referred to as (111) for simplicity) was also measured during the melting and recrystallization experiments to monitor the changes in crystallinity to a first approximation. From Figure 6 it can be seen that the integrated (111) intensity curve mirrors the invariant results. As the sample is heated to

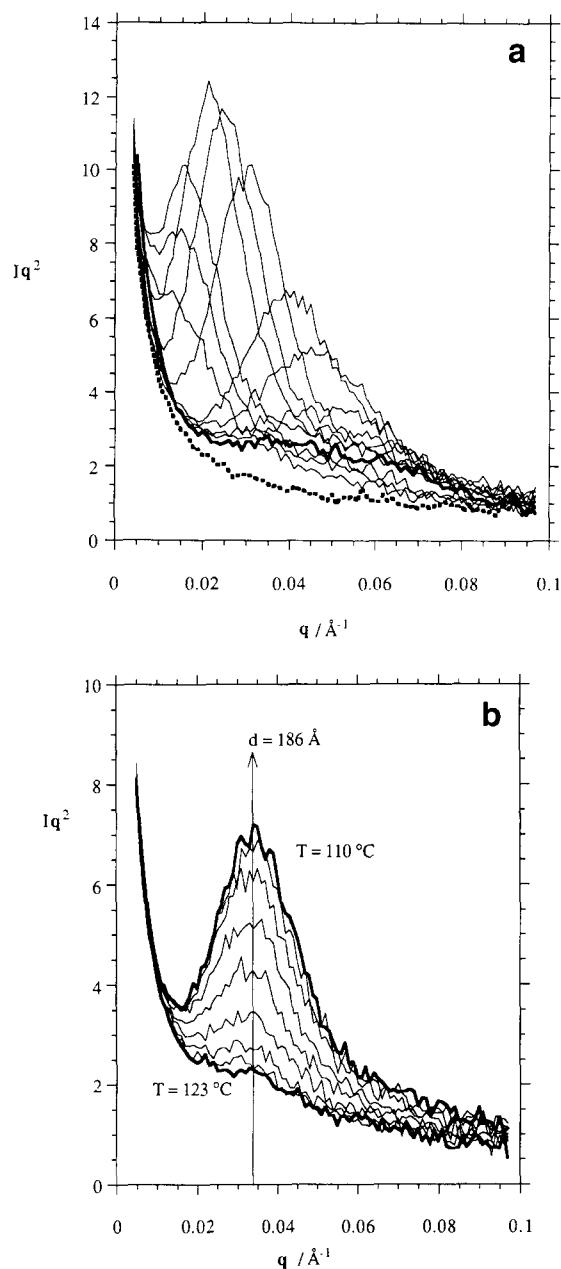


**Figure 5** Selected SAXS patterns of intensity  $I(q)q^2$  versus scattering vector  $q$  ( $0 < q < 0.1 \text{ \AA}^{-1}$ ) (a) in the range  $60\text{--}200^\circ\text{C}$  obtained during the melting of the quenched form of PP and (b) in the range  $123\text{--}110^\circ\text{C}$  obtained during the recrystallization of PP from the melt

above  $60^\circ\text{C}$  the crystallinity increases as the transition from quenched to monoclinic  $\alpha$  modification proceeds. Upon melting the sample becomes amorphous and the crystallinity drops to zero. On recrystallization the crystallinity can be determined by correlating the maximum in the relative invariant curve to the point at which 50% crystallinity occurs in the integrated (111) curve. As the molten state corresponds to 0% crystallinity, a linear plot of integrated WAXS intensity versus crystallinity can be drawn and hence the crystallinity determined at any point during cooling. The sample was found to increase rapidly in crystallinity to 50% and then continue crystallizing at a slower rate, resulting in a sample with an estimated crystallinity of  $\sim 75\%$ . This value is higher than expected, indicating that this method is only approximate, although it can be used to monitor the rate at which the sample crystallizes upon cooling

from the melt. Errors have arisen in the experiment owing to 50% crystallinity being estimated at  $\sim 110^\circ\text{C}$  during recrystallization. When corrections are carried out to account for the coefficient of linear thermal expansion, and to convert volume fraction of crystals to weight fraction, the weight fraction of crystals is estimated at 61%, which is in good agreement with previous findings<sup>2,3</sup>.

The SAXS/WAXS results are reflected in the d.s.c. traces obtained from the melting and recrystallization of a similar sample of PP under comparable conditions (Figure 7). On heating the sample at  $10^\circ\text{C min}^{-1}$ , an exotherm is observed in the range  $65\text{--}120^\circ\text{C}$  (Figure 7a). This corresponds exactly to the region on the WAXS scan over which the transition from quenched to monoclinic occurs. Above  $130^\circ\text{C}$  the PP began to melt and the sample was found to have a melting point peak of  $162^\circ\text{C}$ . On cooling at  $10^\circ\text{C min}^{-1}$ , the sample was found to exhibit a smooth baseline until about  $123^\circ\text{C}$  where crystallization began (Figure 7b). Crystallization was complete at  $103^\circ\text{C}$ , with the peak crystallization temperature  $T_c$  being estimated at  $115^\circ\text{C}$ . Below  $100^\circ\text{C}$  no further transitions were detected by d.s.c.

Analysis of the d.s.c. traces obtained enables the energy involved in the transition from quenched to monoclinic  $\alpha$  modification to be estimated at  $11 \text{ J g}^{-1}$ , which is comparable with the value of  $17 \text{ J g}^{-1}$  obtained by Finchera and Zannetti<sup>16</sup>. Discrepancies in the values obtained may arise from a number of sources, including: (i) different heating rates may have been employed during melting of the samples; (ii) the areas under the curves may have been calculated between different temperature limits; (iii) the initial samples may have been quenched

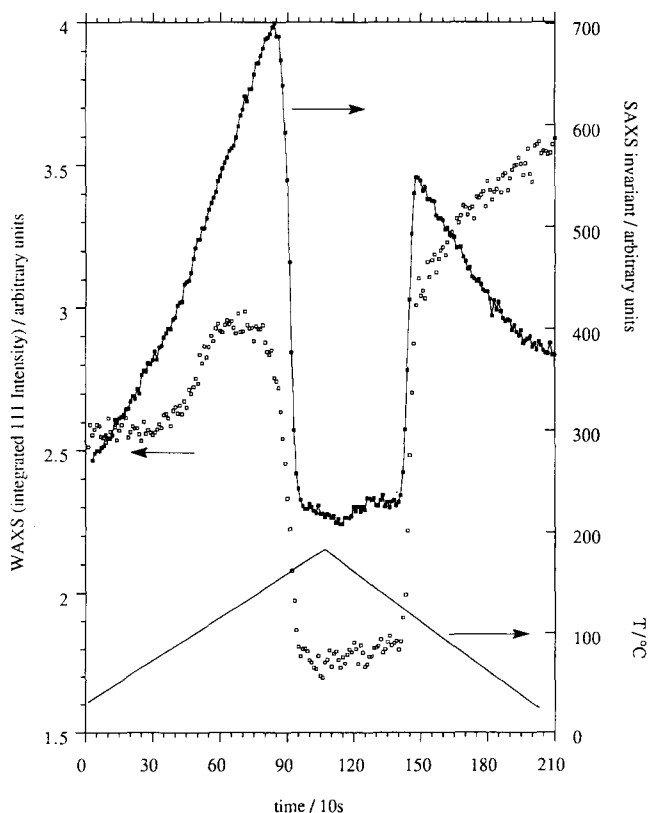


**Figure 6** Relative invariant and integrated WAXS (111) intensity versus time obtained during the melting and recrystallization of the quenched form of PP

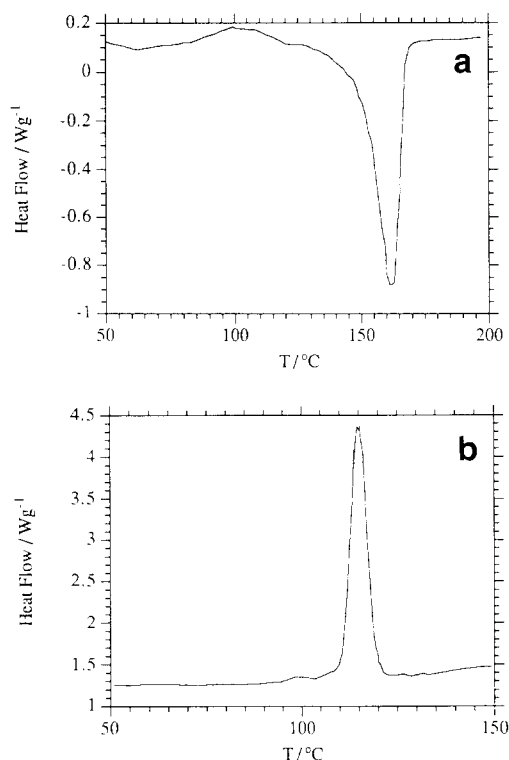


**Figure 7** D.s.c. curves obtained for (a) melting of the quenched form of PP at  $10^{\circ}\text{C min}^{-1}$  and (b) recrystallization of PP from the melt at  $10^{\circ}\text{C min}^{-1}$

to different temperatures, resulting in samples with different thermal histories; and (iv) different grades of material were used (Finchera and Zannetti<sup>16</sup> used PP homopolymer).

It can be concluded that the only transition as evidenced by d.s.c. and WAXS before melting appears to be a solid-state transition from quenched to monoclinic, in agreement with previous results<sup>12–16,18</sup>. This transition, thermally activated, shows that relatively little molecular realignment is required to induce the transition to the monoclinic  $\alpha$  structure (as the movement of the molecular chains is severely restricted in the solid state). These results therefore suggest that the quenched structure is paracrystalline, exhibiting some form of local ordering, possibly of the monoclinic type. Closer examination of the room temperature static WAXS scan (Figure 2) reveals a slight shoulder on the peak at lower angle, probably due to the (110) peak of the monoclinic  $\alpha$  phase. As the peak at lower angle for the quenched form is due to the interatomic vector between adjacent chains<sup>24</sup> and is not related to the stereoregularity of the polymer chains, it therefore seems unlikely that the order within the quenched phase can be explained by the conventional hexagonal structure in PP<sup>3</sup> especially as the nucleation and growth of this phase are more difficult than for the monoclinic phase, which usually occurs only under specialized conditions such as: (i) crystallization from the melt at temperatures in the range  $100\text{--}130^{\circ}\text{C}$ <sup>4</sup>; (ii) crystallization from an oriented melt<sup>25</sup>; or (iii) crystallization from the melt in the presence of nucleating agents<sup>26</sup>.

During processing the cast film is quenched rapidly to prevent crystallization occurring. What little crystallization does occur will be at temperatures of less than  $100^{\circ}\text{C}$ <sup>27</sup>. The casting process essentially freezes a randomly oriented structure into the film, and hence

conditions (i) and (ii) above are not valid. During film manufacture, nucleating agents were not added to the polymer so as to avoid any crystallization processes occurring and thus produce a clear film, and hence condition (iii) is also not fulfilled.

Synchrotron SAXS analysis has been carried out by Forgáes *et al.*<sup>28</sup> to monitor the transition from hexagonal to monoclinic in isotactic PP and they showed that the transition occurs in the range  $130\text{--}150^{\circ}\text{C}$ , which is much higher than the transition temperature range observed in this experiment. Hence it seems very unlikely that the quenched form of PP is related to the hexagonal structure of PP described by Kieth *et al.*<sup>3</sup>.

## CONCLUSIONS

In summary, the WAXS, SAXS and d.s.c. results can all be correlated and used to explain the melting and recrystallization processes occurring in a quenched sample of PP under a given set of conditions. The results for this experiment clearly show that the melting and recrystallization processes can be divided into three distinct stages.

1. The solid-state transition from quenched to monoclinic  $\alpha$  modification occurring in the range  $65\text{--}120^{\circ}\text{C}$ , which results in a sample that is more structured, with a higher crystallinity and hence more long-range order.
2. The continuous annealing and melting of this monoclinic  $\alpha$  modification sample at a temperature of  $162^{\circ}\text{C}$ .
3. Recrystallization of the melt into the monoclinic  $\alpha$  modification in the range  $125\text{--}103^{\circ}\text{C}$ , apparently without any intermediate formation of material with the quenched structure.

## ACKNOWLEDGEMENTS

W. J. O'Kane would like to thank the Department of Education for Northern Ireland (DENI) and the Four Square Division of Mars (GB) Ltd for financial support. R. J. Young is grateful to the Royal Society for support in the form of the Wolfson Professorship in Materials Science. Beam time at Daresbury was provided under Minor Grant J37.

## REFERENCES

- 1 Natta, G. *J. Polym. Sci.* 1955, **16**, 143
- 2 Natta, G. and Corradini, P. *Nuovo Cim. Suppl.* 1960, **15**, 40
- 3 Kieth, H., Padden, F. J., Walter, N. M. and Wyckoff, H. W. *J. Appl. Phys.* 1959, **30**, 1485
- 4 Turner-Jones, A., Aizlewood, J. and Beckett, D. *Makromol. Chem.* 1964, **75**, 134
- 5 Addinck, E. and Bientema, J. *Polymer* 1961, **2**, 185
- 6 Natta, G., Peraldo, M. and Corradini, P. *Rand. Accad. Naz. Lincei* 1959, **26**, 14
- 7 Miller, R. L. *Polymer* 1960, **1**, 135
- 8 Corradini, P., Petraccone, V., De Rosa, C. and Guerra, G. *Macromolecules* 1986, **19**, 2699
- 9 Gailey, J. and Ralston, R. *SPE Trans.* 1964, **4**, 29
- 10 Gesovich, D. and Geil, P. *Polym. Eng. Sci.* 1968, **8**, 202
- 11 Bodor, G., Orell, M. and Kallo, A. *Fraserforsch. Textil-Tech.* 1964, **15**, 527
- 12 Grebowicz, J., Lau, I. F. and Wunderlich, B. *J. Polym. Sci., Polym. Symp. Edn* 1984, **71**, 19
- 13 Glotin, M., Rahalkar, R., Hendra, P., Cudby, M. and Willis, H. *Polymer* 1981, **22**, 731
- 14 Vittoria, V. *J. Macromol. Sci. Phys. B* 1989, **28**(1), 97

SAXS/WAXS and d.s.c. analysis of quenched polypropylene: W. J. O'Kane et al.

- 15 Vittoria, V. *J. Macromol. Sci. Phys. B* 1989, **28**(3/4), 489
- 16 Finchera, A. and Zannetti, R. *Makromol. Chem.* 1975, **176**, 1885
- 17 Boyer, R. F. *J. Macromol. Sci., Phys. B* 1973, **8**(3/4), 503
- 18 Zannetti, R., Celotti, G., Finchera, A. and Francesconi, R. *Makromol. Chem.* 1969, **128**, 137
- 19 Bras, W., Derbyshire, G. E., Ryan, A. J., Mant, G. R., Felton, R. A., Lewis, R. A., Hall, C. J. and Greaves, G. N. *Nucl. Instrum. Meth. Phys. Res.* 1992, in press
- 20 Ryan A. J. *J. Therm. Anal.* 1993, **40**, 887
- 21 Piccarolo, S. *J. Macromol. Sci., Phys. B* 1992, **31**(4), 501
- 22 Baltá-Calleja, F. J. and Vonk, C. G. 'X-ray Scattering of Synthetic Polymers', Elsevier, Amsterdam, 1989, p. 78
- 23 Van Krevelin, D. W. 'Properties of Polymers', Elsevier, Amsterdam, 1990, p. 164
- 24 Ashby, G. E. and Hoeg, D. F. *J. Polym. Sci.* 1959, **39**, 535
- 25 Lovinger, A. J., Chua, J. O. and Gryte, C. C. *J. Polym. Sci., Polym. Phys. Edn* 1977, **15**, 641
- 26 Leugering, H. J. *Makromol. Chem.* 1967, **109**, 204
- 27 O'Kane, W. J. and Young, R. J. unpublished results, 1992
- 28 Forgães, P., Tolochko, B. P. and Sheromov, M. A. *Polym. Bull.* 1979, **1**, 127